DOI 10.1016/j.est.2022.104301
ISSN 2352-152X

Publisher: Elsevier

Journal of Energy Storage 50 (2022) 104301

Contents lists available at ScienceDirect

Journal of Energy Storage

journal homepage: www.elsevier.com/locate/est

Research Papers

A new design of experiment method for model parametrisation of lithium ion battery

Cheng Zhang [a,*], Yue Guo [a], Chongming Wang [a], Shen Li [b], Oliver Curnick [a], Tazdin Amietszajew [a], Rohit Bhagat [a]

[a] Institute for Clean Growth and Future Mobility, Coventry University, CV1 5FB, United Kingdom
[b] Department of Mechanical Engineering, Imperial College London, SW7 2AZ, United Kingdom

ARTICLE INFO

Keywords:
Lithium-ion battery
Equivalent circuit model
Design of experiment
Model parametrisation
SoC estimation

ABSTRACT

Equivalent circuit models (ECMs) have been widely used to describe the electrical dynamics of lithium-ion batteries. A high model accuracy is important for effective simulation and control of the battery system. The model accuracy depends on the design of experiment (DoE) method for battery test and the optimisation approach for ECM parameter identification. While many optimisation approaches have been proposed in literature to identify the parameters, the effect of DoE on the model accuracy is usually overlooked and undervalued. A novel DoE method is proposed in this paper which uses both partial discharge test (PDT) and deep discharge test (DDT) for battery testing. It is shown through careful test data analysis that, the conventional DoE methods using either PDT or DDT cannot capture the battery's dynamics to sufficient accuracy. Experimental data are collected using a commercial lithium ion battery. Results show the new DoE method can significant improve the ECM accuracy, i.e., reducing the root mean square error by ~70% in comparison with conventional DoE approach. In addition, the improved model accuracy contributes to a significant increase in the SoC estimation accuracy using extended Kalman filter.

1. Introduction

Lithium-ion batteries (LIBs) are widely used in electric vehicles and stationary energy storage which play a key role in decarbonizing the transport and energy sectors [1]. A battery management system (BMS) is essential to monitor and control the real-time operation of the battery system to ensure safety and efficiency. To enhance the BMS functionality, a battery model is usually required to predict the system dynamics under various operating conditions [2]. Among different types of models, including electrochemical models, reduced order models and black-box models [3–7], the equivalent circuit model (ECM) is usually favoured for onboard BMS implementation due to its simple structure, ease of parameterisation and desirable accuracy [8–10]. ECM has been widely used for model-based real-time parameter and state estimation of LIBs [9,11–13].

Improving the ECM's accuracy is important for the BMS and the battery system. First, a high ECM accuracy leads to accurate prediction of the battery's power capacity, which is a key parameter for real-time power management of the battery system, e.g. during EV's acceleration and regenerative break [14]. Second, the ECM accuracy affects the estimation accuracy of the battery's internal power loss and heat generation, as well as the resulting temperature rise, which is key to ensuring proper thermal management. Further, ECM-based estimation algorithms such as the extended Kalman filter, unscented Kalman filter, particle filter, etc., have been used for state of charge (SoC) estimation [15–19]. The SoC estimation accuracy depends on the model accuracy [20]. In addition, a high model accuracy is vital in preventing the divergence of the Kalman filter estimation [21].

Design of experiment (DoE) for battery test is usually the first step of ECM development. There are generally two types of DoE methods, i.e. optimal DoE and empirical DoE. Optimal DoE methods aim to optimise the load current profile to maximize parameter identifiability, which is usually measured by the Fisher information matrix. For example, the magnitudes and frequencies of the sine waves of the load current profile

Abbreviations: BMS, battery management system; CC, constant current; CV, constant voltage; DoE, design of experiment; DDT, deep discharge test; ECM, equivalent circuit model; LIB, lithium ion battery; LS, least squares; NPM, new parametrisation method; OCV, open circuit voltage; PDT, partial discharge test; RC, resistor-capacitor; RMSE, root mean square error; SoC, state of charge.

* Corresponding author.
E-mail address: ad4275@coventry.ac.uk (C. Zhang).

https://doi.org/10.1016/j.est.2022.104301
Received 28 October 2021; Received in revised form 12 January 2022; Accepted 20 February 2022
Available online 1 March 2022

were optimised to maximize the parameter identifiability and to improve the ECM accuracy in [22]. Optimal DoE methods have also been applied for parametrising electrochemical models in [23,24]. However, one disadvantage of optimal DoE methods is the high computational expense. Further, the mathematically optimised current profile, e.g., sine waves, may have low relevance with the targeted practical applications, e.g. in EVs. Therefore, the optimal DoE methods are not used in this paper.

The empirical DoE methods include some widely-used current profiles for battery test, such as pulse current [9,25,26], constant current [27–29], multiple sine wave [30], electrochemical impedance spectroscopy [31] and representative drive cycles [32,33]. Here, we focus on discharging test and further categorize these current profiles into two groups, i.e. partial discharge test (PDT) that keeps the battery SoC within a narrow window (e.g. 10% SoC variation) and deep discharge test (DDT) that continuously goes through a wide SoC range, e.g. fully discharge from 100 to 0% SoC at constant current. Since the battery's internal reactions involve highly complex and nonlinear processes, the battery's external electrical properties, such as impedance and resistance, depend on the load current profile [34]. Therefore, the PDT and DDT can reveal different properties of the battery. However, this effect is often overlooked in literature, and many DoE methods use either PDT or DDT for battery test and ECM parametrisation. This leads to poor generalisation performance of the obtained ECM. This paper will demonstrate that it is essential to use both PDT and DDT in order to capture the battery's dynamics to sufficient accuracy.

On the other hand, although using DDT data for battery test can improve the model accuracy, it also introduces a challenge to model parameter optimisation. This is because the ECM's parameters depend on SoC. The most popular method to deal with this parameter dependency is to 'divide and conquer', i.e., to identify the parameters at each SoC level separately to reduce complexity [9,30,32]. This results in a family of local models, which can then be interpolated to capture the parameter dependency. However, this method cannot apply to DDT because the test goes continuously through a wide range of SoC, and the parameters under these SoC levels become coupled. Although a nonlinear global optimisation method can be used to optimise all the parameters together [28,35,36], the computational cost is high due to the high parameter dimension, and the probability of finding global minima is low. To address this issue, a recently developed algorithm by the authors [37] is used in this paper to capture the parameter dependency on SoC. The method has several advantages: low optimisation complexity, applicability to a wide range of operating conditions, smooth parameter transition, and improved model accuracy, which have been validated by experimental data [37].

The contribution of this paper is summarised as follows. A novel DoE method for battery test and ECM parametrisation is proposed in this paper. Although DoE has a high impact on ECM accuracy, this issue is generally overlooked and undervalued in literature. Through careful analysis of the experimental data collected on a LIB cell, this paper shows that the widely used battery test method, using either PDT or DDT, cannot capture the battery's dynamics to sufficient accuracy. To address this issue, the proposed DoE method combines PDT and DDT for battery test. Experimental results show that the new DoE method can capture both the transient and steady-state properties of the battery, and significantly improve the ECM accuracy, as well as the SoC estimation accuracy.

This paper is organized as follows. Section 2 introduces the ECM. Test data are presented in Section 3. Section 4 explains the parameter optimisation algorithm. Experimental results of modelling and SoC estimation are analysed in Section 5. Section 6 concludes the paper.

2. Battery ECM

The ECM, shown in Fig. 1, includes open circuit voltage (OCV), a series resistor R_0 and several resistor-capacitor (RC) pairs for capturing the battery's internal voltage drop resulting from current excitation [38]. The battery OCV can be measured directly using galvanostatic intermittent titration technique (GITT) or a low-rate constant current discharge test [39], while the RC values need to be identified by fitting the model's voltage prediction to measurements.

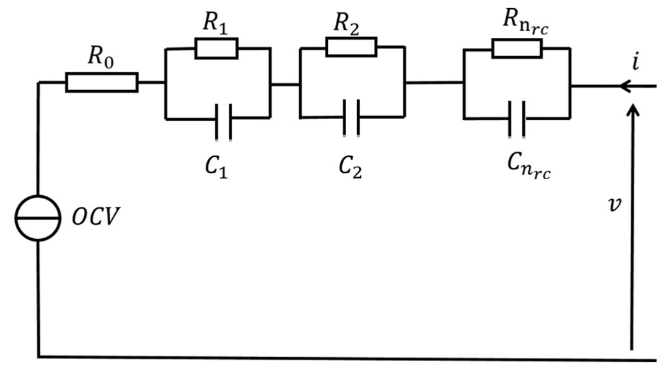

Fig. 1. Battery ECM.

In Fig. 1, v, i represent the battery terminal voltage and current, respectively. Denote n_{rc} as the number of RC networks. Define i_j, v_j, $j = 1, 2, \ldots, n_{rc}$ as the current and overpotential across R_j. Let $\tau_j = R_jC_j$ be the time constant. Assuming the RC parameters and the current keep constant between two data samples, where T_s is the sampling interval in seconds, the dynamics of the RC networks can be formulated as follows,

$$v_j(k+1) = a_jv_j(k) + R_j(1-a_j)i(k), \quad j = 1,2,\ldots,n_{rc} \tag{1}$$

where

$$a_j = exp(-T_s/\tau_j)$$

and k stands for sample time.

Note that this formulation is slightly different from the previous work in [37]. The formulation in [37] is: $i_j(k+1) = a_ji_j(k) + (1 - a_j)i(k)$, and $v_j = R_ji_j$. According to the authors' experience, the new formulation in Eq. (1) improves the stability of SoC estimation in comparison with that in [37]. This effect is explained with more details in the Supplementary material.

Define the total voltage drop across all the RC networks as

$$v_{rc}(k) = \sum_{j=1}^{n_{rc}} v_j(k) \tag{2}$$

The battery SOC is obtained using the widely employed coulomb counting method [9,32],

$$SoC(k+1) = SoC(k) + \frac{T_s}{3600C_n}i(k) \tag{3}$$

where C_n in Ampere-hour is the battery's nominal capacity at 25 °C. Battery C-rate is used to represent the current magnitude, i.e., C − rate = i/C_n. Note that positive current stands for charging.

Next, the battery terminal voltage can be expressed as,

$$v(k) = OCV(k) + R_0i(k) + v_{rc}(k) \tag{4}$$

3. Test data analysis

3.1. Battery test procedure

The battery selected in this paper is a 3.1 Ah, cylindrical 18650 LIB cell (Panasonic NCR18650BD) with NMC Cathode and Graphite Anode, using EC-DC with $LiPF_6$ salt as electrolyte. A Biologic VMP3 battery cycler is used for charging/discharging the cell, which is placed inside a Binder thermal chamber for maintaining the ambient temperature at constant 25 °C. A K-type thermocouple is attached to the battery surface at the cell's middle height for temperature monitoring. The same constant current (CC) constant voltage (CV) procedure is always used to fully charge the battery, i.e. CC charging at 1A to 4.2 V followed by CV phase until the current drops to 50 mA. Discharging tests include PDT (i.e. pulse test in Fig. 2(1a)) and DDT (i.e. CC test at 0.5C in Fig. 2(2a)). In addition, two drive cycle tests are conducted with average current at 0.5C (Fig. 8 in Appendix A). The PDT in Fig. 2(1a) consists of in total 20 steps. Each step starts with three short pulses, i.e., 10-second pulses at 1A, 2A and 3A in turn with a short 10-second rest after each pulse. Next is a long pulse at C/2 that reduces the battery's SoC by 5%, followed by 1-hour rest period.

3.2. OCV and R_0 characterization

The battery's voltage at end of the one-hour rest period in the pulse test in Fig. 2(1a) is taken as the OCV. The ohmic resistance R_0 is calculated as follows using the current jumps in the pulse test,

$$R_0 = \frac{v(k+1) - v(k)}{i(k+1) - i(k)}, \text{if } |i(k+1) - i(k)| > i_{th} \tag{5}$$

where $i_{th} = 0.2C$ is the threshold value. Note that there are several current jump points in each pulse test step, and the R_0 values calculated at these points are slightly different (relatively error within 1%). Therefore, the average value is used as R_0.

3.3. Resistance of the RC networks

Once the battery's OCV and R_0 are characterized, from Eq. (4), the total voltage drop across all the RC networks can be calculated, i.e. $v_{rc} = v - OCV - R_0 i$. Define the effective total resistance of the RC networks as follows,

$$R_{eff} = \frac{v_{rc}}{i} \tag{6}$$

Using the PDT and DDT data, the R_{eff} versus SoC is plotted in Fig. 3. The DDT shows the steady-state R_{eff}, which is a useful indicator of the total resistance of the RC networks. For ECM parameter identification, this total resistance needs to be split into the RC branches with different time constants. The split ratio mainly depends on the transient response of the battery. Therefore, the PDT data, which shows the transient dynamics of R_{eff}, is essential to identify the RC parameters at each SoC level. Fig. 3 clearly shows that the split ratio varies with SoC. Therefore, the PDT and DDT reveal different and complementary properties of the battery, and these two test profiles are both required in order to capture the battery's transient and steady-state responses.

4. Parameter optimisation method

This section presents the parameter optimisation method. To reduce the optimisation complexity, the RC time constants are set to be invariant. The RC time constants mainly represent the time scale of

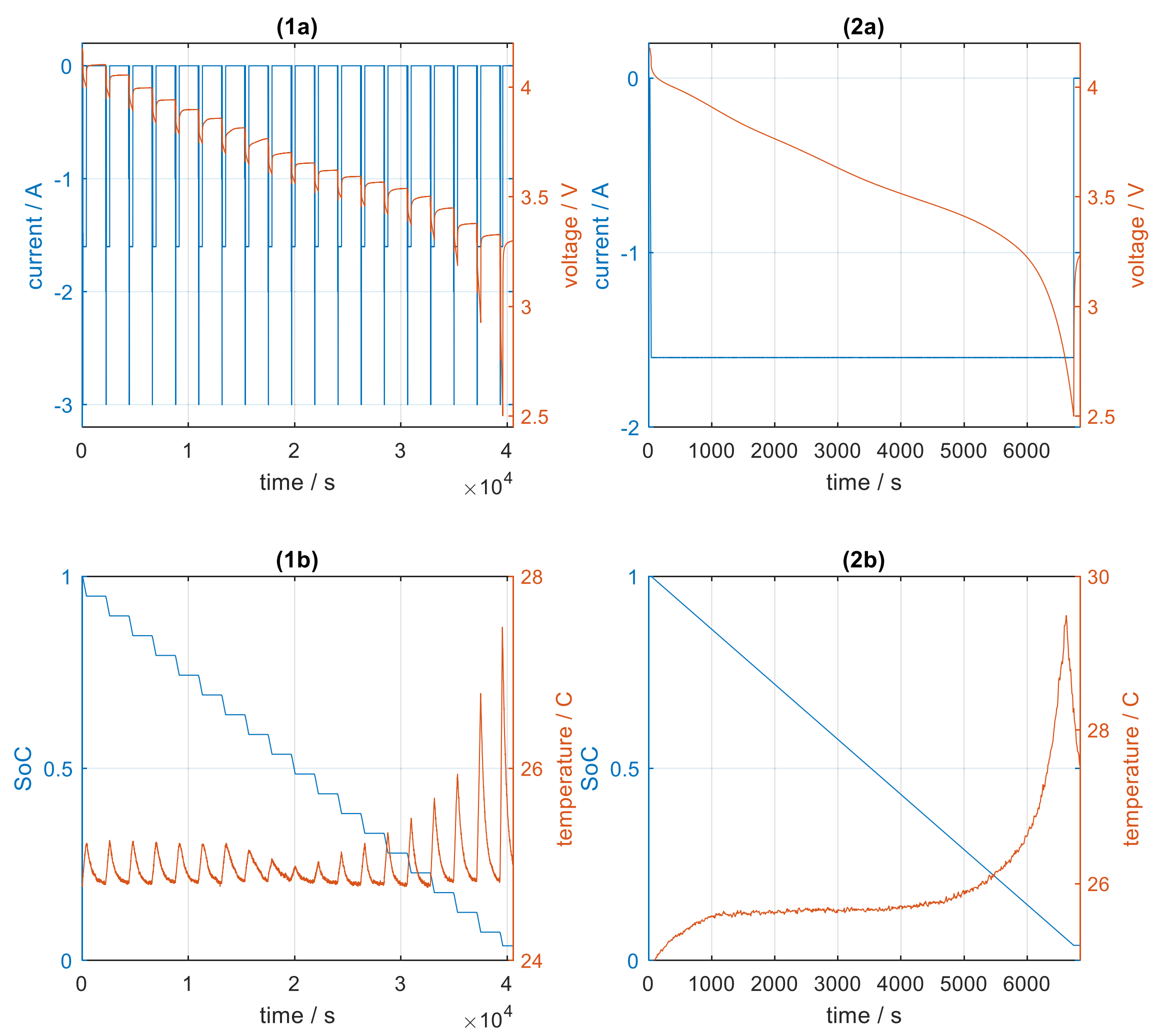

Fig. 2. Battery discharge test. (1a) Pulse test: current and voltage; (1b) pulse test: SoC and battery surface temperature; (2a) CC test: current and voltage; (2b) CC test: SoC and battery surface temperature.

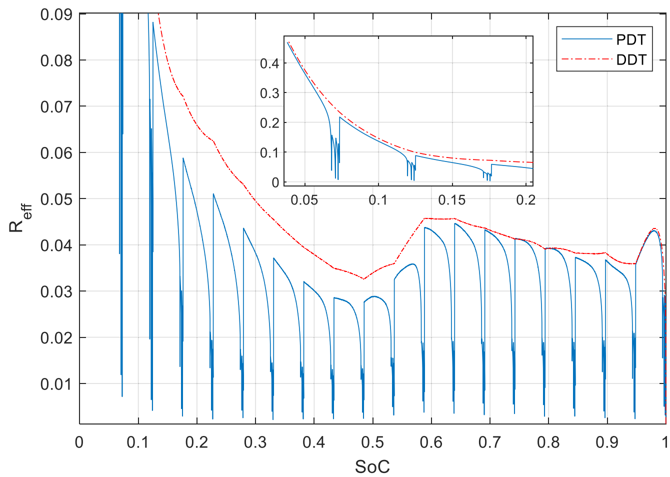

Fig. 3. The total resistance of the RC breaches R_{eff} versus SoC using the PDT and DDT data.

interest when capturing the voltage dynamics, which can be considered independent from the SoC.

The following SoC breakpoints are used to describe the parameter dependency on SoC,

$$0 \le SoC_1 < SoC_2 < \ldots < SoC_{n_{soc}} \le 100\% \tag{7}$$

where n_{soc} is the number of SoC breakpoints.

It is widely known that ECM has difficulty to capture the highly nonlinear dynamics of LIBs in the low SoC range. To improve the model accuracy in the low SoC range, a new model structure needs to be adopted [40]. Since this paper focuses on DoE method, the parameter optimisation is performed at 20–100% SoC. One advantage of limiting the SoC range is that, as it is shown in Figs. 2 and 8, the battery's temperature rise during 20–100% SoC is less than 1.2 °C. Therefore, the temperature effect on the ECM's parameters can be neglected in this paper.

Next, define the dependency of the resistor value on the SoC as follows,

$$R_j(SoC) = \sum_{m=1}^{n_{soc}} R_{j,m} f_m(SoC), j = 1, 2, \ldots, n_{rc} \tag{8}$$

where $R_{j,\,m}$ is the constant coefficient and f_m is the base function at each SoC breakpoint. A linear interpolation function is used in this paper as the base function.

Substitute Eq. (8) into Eq. (1), yielding,

$$v_j(k+1) = a_j v_j(k) + \sum_{m=1}^{n_{soc}} R_{j,m} f_m(SoC)\left(1 - a_j\right) i(k), j = 1, 2, \ldots, n_{rc} \tag{9}$$

Since a_j is constant, Eq. (9) represents a linear system. Denote,

$$q_{j,m}(k+1) = a_j q_{j,m}(k) + \left(1 - a_j\right) f_m(SoC) i(k), j = 1, 2, \ldots, n_{rc} \tag{10}$$

Then

$$v_j = \sum_{m=1}^{n_{soc}} R_{j,m} q_{j,m}, j = 1, 2, \ldots, n_{rc}$$

Note that here the time step symbol k is dropped for simplicity. Substitute the above equation into Eq. (4), yielding

$$v - OCV - R_0 i = \sum\nolimits_{j=1}^{n_{rc}} \sum_{m=1}^{n_{soc}} R_{j,m} q_{j,m} \tag{11}$$

Denote

$$\begin{aligned} y &= v - OCV - R_0 i \\ r &= \left[R_{1,1}, R_{1,2}, \ldots, R_{1,n_{soc}}, \ldots, R_{n_{rc},1}, R_{n_{rc},2}, \ldots, R_{n_{rc},n_{soc}}\right]^T \\ q &= \left[q_{1,1}, q_{1,2}, \ldots, q_{1,n_{soc}}, \ldots, q_{n_{rc},1}, q_{n_{rc},2}, \ldots, q_{n_{rc},n_{soc}}\right]^T \end{aligned} \tag{12}$$

where the superscript T stands for transpose. From Eq. (11) we get,

$$y = q^T r$$

Given a set of the time constants, $\tau_1 < \tau_2 < \ldots < \tau_{nrc}$, and the current profile i, the elements in vector q can be calculated using Eq. (10). Denote the value of y and q at sample step k as $y(k)$ and $q(k)$, respectively, and let

$$Y = \begin{bmatrix} y(1) \\ y(2) \\ \ldots \\ y(N) \end{bmatrix}, Q = \begin{bmatrix} q^T(1) \\ q^T(2) \\ \ldots \\ q^T(N) \end{bmatrix}$$

where N is the total number of data samples. Then from Eq. (11) we obtain a least-squares formulation as follows,

$$Y = Qr \tag{13}$$

The optimal solution of r to Eq. (13), $\hat{r}$ can be obtained using least-squares solvers. This is a convex optimisation problem which can be solved efficiently, and if necessary, constraints can be introduced to ensure a smooth transition of R_j across SoC levels. The Matlab solver 'lsqlin' is used in this paper for finding the optimal resistor values in Eq. (13).

Next, the voltage fitting error can be calculated as follows,

$$E = Y - Q\hat{r} \tag{14}$$

and the model's voltage RMSE is $\sqrt{\frac{1}{N}E^T E}$. Note that this RMSE depends on the RC time constants, τ_j. The optimal τ_j can then be found by solving the following nonlinear parameter optimisation problem

$$\min_{\tau_1, \tau_2, \ldots, \tau_{nrc}} \sqrt{\frac{1}{N} E^T E} \tag{15}$$

This parametrisation method can take more than one test data set (e.g. PDT and DDT test data) for parameter optimisation. The test data will be concatenated to form a single Y and Q matrix in Eq. (13).

With only a couple of time constant parameters to optimise (generally 2 to 4), the chance of finding global minimum is greatly increased compared with optimising all the model parameters together using the Genetic algorithm [41]. The Matlab solver 'fmincon' is used in this paper for finding the optimal RC time constants in Eq. (15).

5. Experimental results

As a comparison to the NPM, the RC parameters are also optimised using a conventional least squares (LS) method as in [9,26] (the benchmark method), where a single discharge pulse is used for identifying the RC parameters at each SoC level. The parameter dependency on SoC is described using the linear interpolation method.

For the proposed new parametrisation method (NPM), two cases are considered to compare the new DoE method with the conventional DoE method that only uses PDT for battery test. The first case uses only PDT for model parametrisation, and the second case uses both PDT and DDT data.

Therefore, in total, three parametrisation methods are compared in this section. Denote 'LS + p' as the LS method with the pulse discharge data, 'NPM + p' as the NPM with the pulse discharge data, and 'NPM + p + cc' as the NPM with both the pulse and CC discharge data.

Considering that the battery shows different dynamics between underload and rest period which require different model parameters [37], only the underload data are used for model training. Following the same procedure in [37], the number of RC networks is set to be three.

5.1. Model validation

The model validation results using the pulse discharge data from 20% to 100% SoC are shown in Fig. 4. The RMSE of the model's voltage prediction are in turn 2.92 mV, 4.73 mV and 4.68 mV for the three methods, ‘LS + p’, ‘NPM + p’ and ‘NPM + p + cc’. The modelling results are comparable mainly because this pulse test data is used for model training in all three cases. The models show higher voltage error during the relaxation stage than underload, as shown in Fig. 4(b). This is because only the underload data is used for model training.

The model validation results using the CC discharge test data from 20% to 100% SoC are shown in Fig. 5. The RMSE for these three methods (‘LS + p’, ‘NPM + p’, ‘NPM + p + cc’) are in turn 21.8 mV, 4.81 mV and 0.854 mV. In comparison with the ‘NPM + p’ and ‘LS + p’ methods, the proposed ‘NPM + p + cc’ method reduced the RMSE by more than 80% and 95%, respectively. This is mainly because the new DoE method can more accurately capture the voltage transition between SoC levels, as it is shown in Fig. 5(b) from 3000 s to 5800 s, while the conventional DoE method that uses only PDT data shows high voltage error under this continuous CC discharge test.

The model validation results using the drive cycle discharge data set 1 in Fig. 8(1a) from 20% to 100% SoC are shown in Fig. 6. Note that this data set is not used for model training in all three cases. Therefore, the model's generalisation performance is compared here. The RMSE for the three methods (‘LS + p’, ‘NPM + p’, ‘NPM + p + cc’) are in turn 20.8 mV, 4.8 mV and 1.91 mV. In comparison with the ‘LS + p’ and ‘NPM + p’ methods, the proposed ‘NPM + p + cc’ method reduced the model error by about 90% and 60%, respectively. This is mainly because the proposed DoE method can better capture the transition effect between neighbouring SoC levels, and this drive cycle test goes continuously through a wide SoC window. The new DoE method achieved noticeably higher model accuracy by eliminating the bias error in Fig. 6(b) from 3500 s to 5500 s.

The model's generalisation capability is a critical performance indicator for practical implementation. The above validation results show that the proposed NPM with the new DoE achieves noticeably higher model accuracy and better generalisation performance in a new data set that is not used during model training. The root cause is that the battery is a complex nonlinear system, and the parameters of the simplified ECM

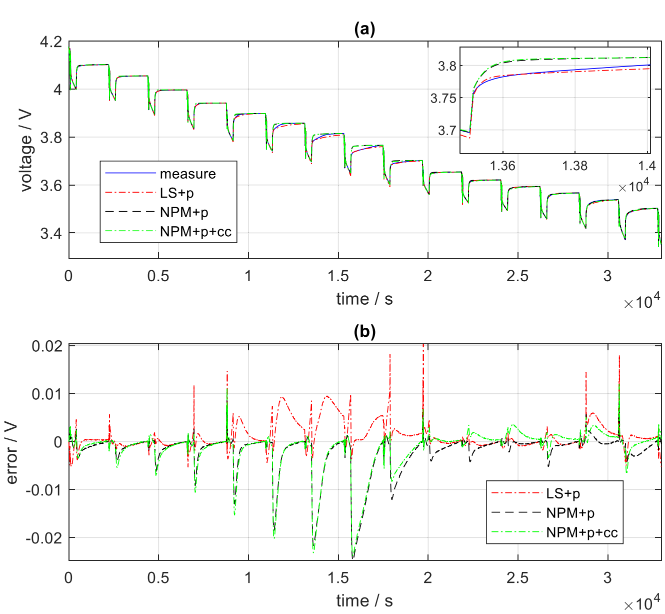

Fig. 4. Model validation results using the pulse discharge data.

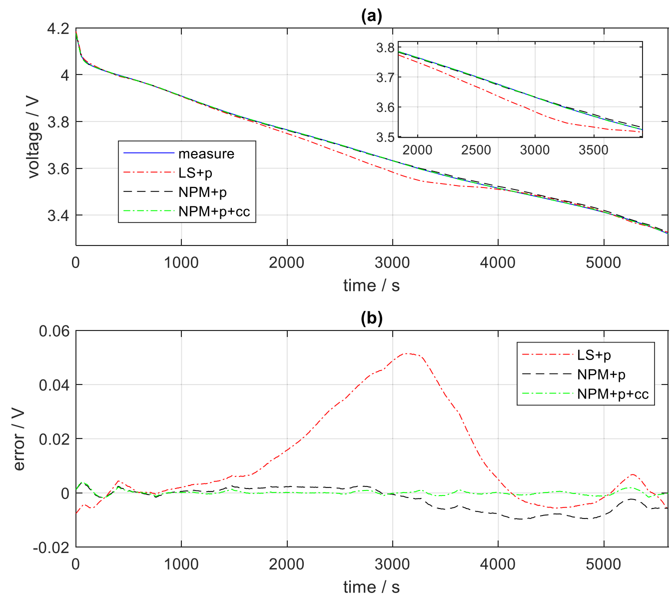

Fig. 5. Model validation results using the CC discharge test data.

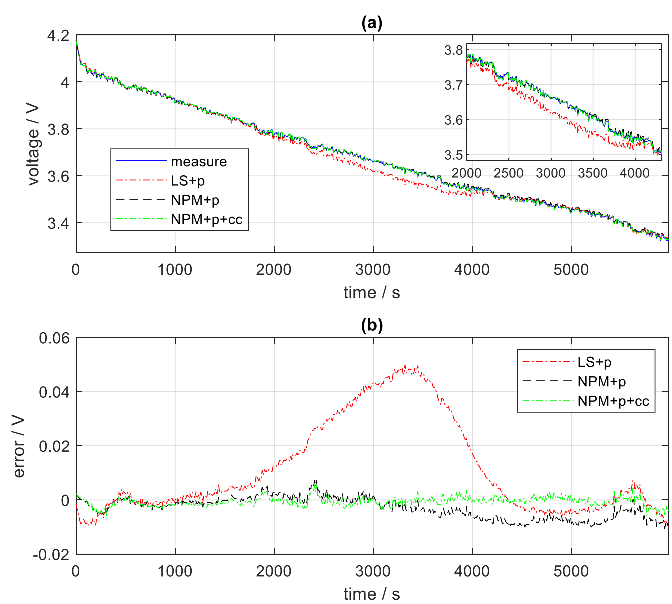

Fig. 6. Model validation results using the drive cycle discharge test data set 1.

are dependent on the load profile, and the PDT and DDT are the two most common load profiles in EV applications.

5.2. SoC estimation results

The ECM-based SoC estimation performance is also compared using the three parameterisation methods. The drive cycle test data set 2 in Fig. 8(2a) from 20% to 100% SoC are used here.

Since the model structure is the same and only the parameters are different, the same extended Kalman filter (EKF) is applied for a fair comparison. The EKF has been widely used in literature for battery SoC estimation. Klintberg et al. has shown that if model uncertainties are ignored, EKF already achieves a close-to-optimal estimation accuracy (i.e. close to the so-called Cramer-Rao lower bound) [42]. The same EKF implementation procedure in [32] is followed here, and therefore the EKF equations are omitted.

The same initial condition is applied in all three cases. The initial guess of SoC is 95%, with 5% SoC error. The initial voltage over the RC networks is set to 0 V. The initial state estimation covariance matrix is set as *diag*([1e-4, 1e-4, 1e-4, 1e-4]), where '*diag*' is the Matlab command to generate diagonal matrix from the input vector. The process noise covariance matrix is diag([1e-7, 1e-10, 1e-10, 1e-10]) and the measurement covariance matrix is 9e-6.

The SoC estimation results are shown in Fig. 7. Since the model structure and the initial conditions of the EKF are the same, the three methods achieved similar convergence rate, as shown in Fig. 7(a). The RMSEs of SoC estimation for the three methods ('LS + p', 'NPM + p', 'NPM + p + cc') are in turn 2.74%, 0.774% and 0.616%. In comparison with the 'LS + p' and 'NPM + p' methods, the proposed 'NPM + p + cc' method reduced the SoC estimation error by about 77% and 20%, respectively. Further, it can be seen in Fig. 7(b), the proposed DoE method, 'NPM + p + cc', effectively eliminated the bias error in SoC estimation from 3500 s to 5000 s, while the conventional DoE methods ('LS + p' and 'NPM + p') showed high bias error.

Finally, by comparing the SoC estimation results with the modelling results in Figs. 5 and 6, it is evident that the SoC estimation accuracy is closely related to the ECM accuracy, which reiterates the importance of improving the ECM accuracy through the novel DoE and NPM proposed in this paper.

6. Conclusion

Equivalent circuit model (ECM) is widely used for simulation and control of lithium ion battery systems. The model accuracy is key to its success in practical implementation. Apart from model parameter optimisation, design of experiment (DoE) for battery test also has a high impact on the ECM accuracy. However, this effect is generally overlooked in literature leading to low model performance. To address this issue, this paper develops a novel DoE method for battery test by combining two complementary load profiles, i.e., partial discharge test (PDT) and deep discharge test (DDT). While many existing DoE methods use either PDT or DDT for battery test, the test data analysis in this paper shows only a combination of PDT and DDT can capture the battery's dynamics with sufficient accuracy. The experimental results confirm that the proposed DoE method can significantly improve the ECM accuracy and reduce the modelling root mean square error (RMSE) by ~70% in comparison with the benchmark conventional DoE approach. The improved model accuracy in turn leads to a significant increase of the SoC estimation accuracy by ~70%. This work highlights the importance of proper DoE for ECM parametrisation. Since the ECM and SoC estimation accuracy is key to effective simulation and control of battery systems, and the two load profiles under study (PDT and DDT) are most common battery usage, this work should be of interest to academic and industrial researchers in area of battery energy storage.

Since this work focuses on the novel DoE method, to limit the scope, the effect of temperature, current rate on the ECM parameters is not considered in this paper. However, the developed DoE and model parametrisation algorithm can apply to different temperature levels and current rates to take into consideration of the parameter dependency on these factors. Future work will address these aspects.

CRediT authorship contribution statement

Cheng Zhang: Formal analysis, Writing - original draft.
Yue Guo: Supervision and Resources.
Chongming Wang: Writing - review & editing.
Shen Li: Conceptualization, review.
Oliver Curnick: Writing - review & editing.
Tazdin Amietszajew: Data curation.
Rohit Bhagat: Supervision and Resources.

Declaration of competing interest

The authors declare that they have no known competing financial interests or personal relationships that could have appeared to influence the work reported in this paper.

Appendix A

This section presents the two sets of drive-cycle test data used for validating the model and SoC estimation algorithms in Section 5.

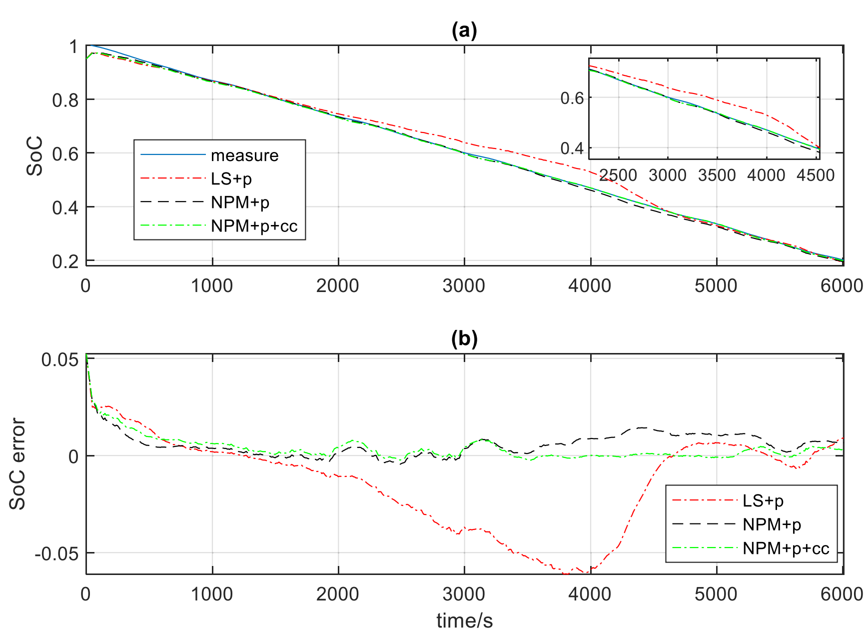

Fig. 7. Comparison of SoC estimation results of the three parametrisation methods using the test data in Fig. 8(2a).

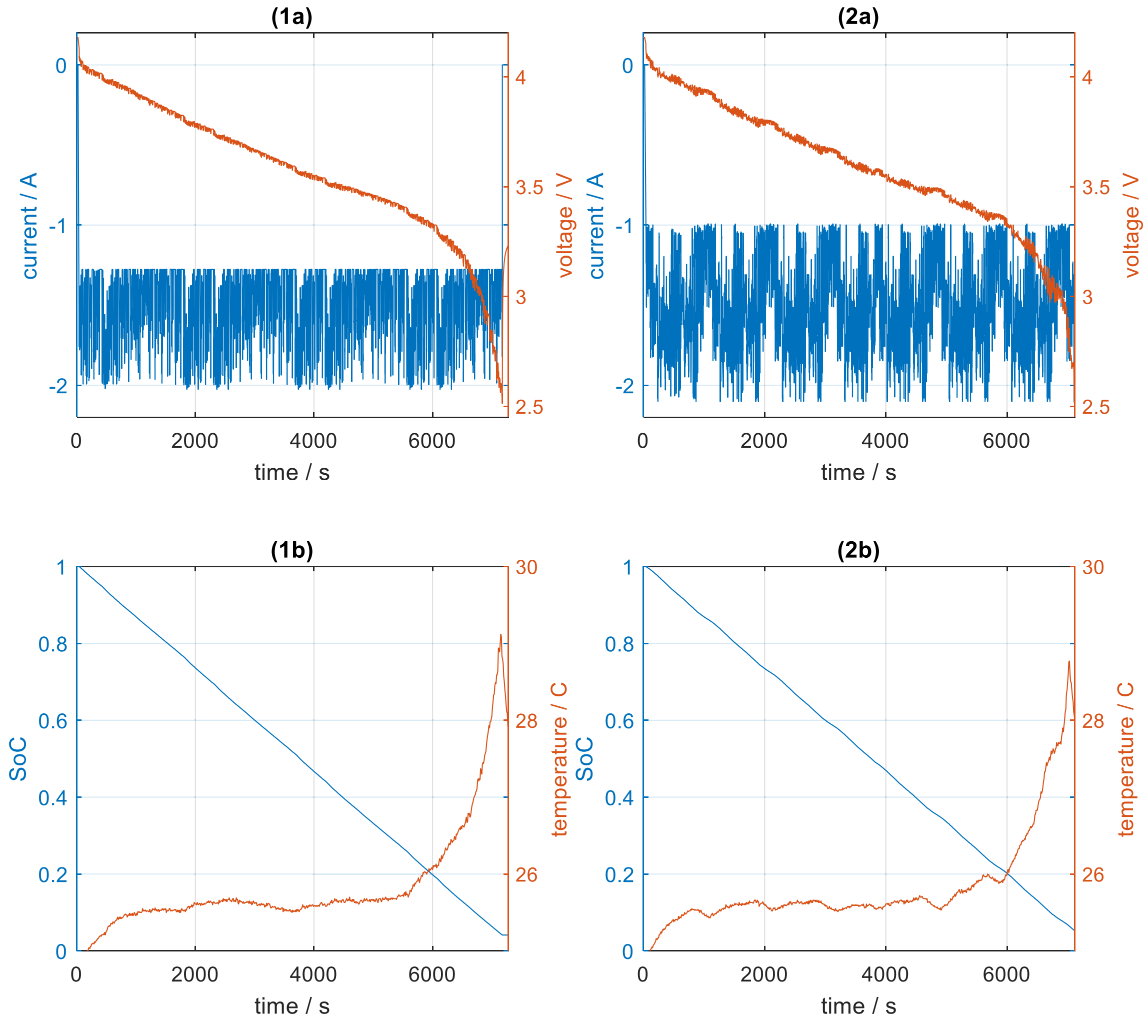

Fig. 8. Battery discharge test. (1a) Drive cycle 1: current and voltage; (1b) drive cycle 1: SoC and battery surface temperature; (2a) drive cycle 2: current and voltage; (2b) drive cycle 2: SoC and battery surface temperature.

Appendix B. Supplementary data

A comparison of the two ways to formulate the dynamic equation of RC network. Supplementary data to this article can be found online at https://doi.org/10.1016/j.est.2022.104301.

References

[1] IEA, Global EV Outlook 2021, Int. Energy Agency, 2021.
[2] L. Lu, X. Han, J. Li, J. Hua, M. Ouyang, A review on the key issues for lithium-ion battery management in electric vehicles, J. Power Sources 226 (2013) 272–288.
[3] C. Zhang, K. Li, S. McLoone, Z. Yang, Battery modelling methods for electric vehicles-a review, in: European Control Conference (ECC), 2014, 2014, pp. 2673–2678.
[4] A. Seaman, T.-S. Dao, J. McPhee, A survey of mathematics-based equivalent-circuit and electrochemical battery models for hybrid and electric vehicle simulation, J. Power Sources 256 (2014) 410–423.
[5] J. Hong, Z. Wang, W. Chen, L.-Y. Wang, C. Qu, Online joint-prediction of multi-forward-step battery SOC using LSTM neural networks and multiple linear regression for real-world electric vehicles, J. Energy Storage 30 (2020), 101459.
[6] L. Li, et al., Lithium-ion battery cathode and anode potential observer based on reduced-order electrochemical single particle model, J. Energy Storage 44 (2021), 103324, https://doi.org/10.1016/j.est.2021.103324.
[7] M. Dubarry, G. Baure, C. Pastor-Fernández, T.F. Yu, W.D. Widanage, J. Marco, Battery energy storage system modeling: a combined comprehensive approach, J. Energy Storage 21 (2019) 172–185, https://doi.org/10.1016/j.est.2018.11.012.
[8] H. He, R. Xiong, H. Guo, S. Li, Comparison study on the battery models used for the energy management of batteries in electric vehicles, Energy Convers. Manag. 64 (2012) 113–121.
[9] C. Zhang, K. Li, L. Pei, C. Zhu, An integrated approach for real-time model-based state-of-charge estimation of lithium-ion batteries, J. Power Sources 283 (2015) 24–36.
[10] R. Guo, W. Shen, A review of equivalent circuit model based online state of power estimation for lithium-ion batteries in electric vehicles, Vehicles 4 (1) (2022) 1–29.
[11] X. He, B. Sun, W. Zhang, X. Fan, X. Su, H. Ruan, Multi-time scale variable-order equivalent circuit model for virtual battery considering initial polarization condition of lithium-ion battery, Energy 244 (2022), 123084, https://doi.org/10.1016/j.energy.2021.123084.
[12] P.P. Mishra, M. Garg, S. Mendoza, J. Liu, C.D. Rahn, H.K. Fathy, How does model reduction affect lithium-ion battery state of charge estimation errors? Theory and experiments, J. Electrochem. Soc. 164 (2) (2017) A237–A251.
[13] F. Sun, R. Xiong, H. He, A systematic state-of-charge estimation framework for multi-cell battery pack in electric vehicles using bias correction technique, Appl. Energy 162 (2016) 1399–1409, https://doi.org/10.1016/j.apenergy.2014.12.021.
[14] G.L. Plett, High-performance battery-pack power estimation using a dynamic cell model, IEEE Trans. Veh. Technol. 53 (5) (2004) 1586–1593.
[15] R.D. Anderson, R. Zane, G. Plett, D. Maksimovic, K. Smith, M.S. Trimboli, Life balancing–a better way to balance large batteries, in: SAE Technical Paper, 2017.
[16] D. Zhou, K. Zhang, A. Ravey, F. Gao, A. Miraoui, Online estimation of lithium polymer batteries state-of-charge using particle filter-based data fusion with multimodels approach, IEEE Trans. Ind. Appl. 52 (3) (2016) 2582–9994.
[17] C. Zhang, L.Y. Wang, X. Li, W. Chen, G.G. Yin, J. Jiang, Robust and adaptive estimation of state of charge for lithium-ion batteries, IEEE Trans. Ind. Electron. 62 (8) (2015) 4948–4957, https://doi.org/10.1109/TIE.2015.2403796.

[18] G.L. Plett, Sigma-point Kalman filtering for battery management systems of LiPB-based HEV battery packs: part 2: simultaneous state and parameter estimation, J. Power Sources 161 (2) (2006) 1369–1384.
[19] S. Wang, C. Fernandez, C. Yu, Y. Fan, W. Cao, D.-I. Stroe, A novel charged state prediction method of the lithium ion battery packs based on the composite equivalent modeling and improved splice Kalman filtering algorithm, J. Power Sources 471 (2020), 228450.
[20] P. Shrivastava, T.K. Soon, M.Y.I. Bin Idris, S. Mekhilef, Overview of model-based online state-of-charge estimation using Kalman filter family for lithium-ion batteries, Renew. Sust. Energ. Rev. 113 (2019), 109233, https://doi.org/10.1016/j.rser.2019.06.040.
[21] Q. Wang, J. Wang, P. Zhao, J. Kang, F. Yan, C. Du, Correlation between the model accuracy and model-based SOC estimation, Electrochim. Acta 228 (2017) 146–159, https://doi.org/10.1016/j.electacta.2017.01.057.
[22] J. Liu, M. Rothenberger, S. Mendoza, P. Mishra, Y. Jung, H.K. Fathy, Can an identifiability-optimizing test protocol improve the robustness of subsequent health-conscious lithium-ion battery control? An illustrative case study, in: 2016 American Control Conference (ACC), 2016, pp. 6320–6325.
[23] S. Mendoza, M. Rothenberger, J. Liu, H.K. Fathy, Maximizing parameter identifiability of a combined thermal and electrochemical battery model via periodic current input optimization, IFAC-PapersOnLine 50 (1) (2017) 7314–7320.
[24] S. Park, D. Kato, Z. Gima, R. Klein, S. Moura, Optimal experimental design for parameterization of an electrochemical lithium-ion battery model, J. Electrochem. Soc. 165 (7) (2018) A1309–A1323.
[25] C. Campestrini, Practical Feasibility of Kalman Filters for the State Estimation of Lithium-ion Batteries, Technische Universität München, 2018. PhD thesis.
[26] S. Thanagasundram, R. Arunachala, K. Makinejad, T. Teutsch, A. Jossen, A cell level model for battery simulation, in: European Electric Vehicle Congress, 2012, pp. 1–13.
[27] M. Lenz, D. Jöst, F. Thiel, S. Pischinger, D.U. Sauer, Identification of load dependent cell voltage model parameters from sparse input data using the mixed integer distributed ant colony optimization solver, J. Power Sources 437 (2019), 226880, https://doi.org/10.1016/j.jpowsour.2019.226880.
[28] J. Brand, Z. Zhang, R.K. Agarwal, Extraction of battery parameters of the equivalent circuit model using a multi-objective genetic algorithm, J. Power Sources 247 (2014) 729–737.
[29] S.K. Rahimian, S. Rayman, R.E. White, Comparison of single particle and equivalent circuit analog models for a lithium-ion cell, J. Power Sources 196 (20) (2011) 8450–8462.
[30] W.D. Widanage, et al., Design and use of multisine signals for li-ion battery equivalent circuit modelling. Part 2: model estimation, J. Power Sources 324 (2016) 61–69.
[31] P. Vyroubal, T. Kazda, Equivalent circuit model parameters extraction for lithium ion batteries using electrochemical impedance spectroscopy, J. Energy Storage 15 (2018) 23–31, https://doi.org/10.1016/j.est.2017.10.019.
[32] C. Zhang, K. Li, J. Deng, S. Song, Improved realtime state-of-charge estimation of LiFePO4 battery based on a novel thermoelectric model, IEEE Trans. Ind. Electron. 64 (1) (2017) 654–663.
[33] H.P.G.J. Beelen, H.J. Bergveld, M.C.F. Donkers, On experiment design for parameter estimation of equivalent-circuit battery models, in: 2018 IEEE Conference on Control Technology and Applications (CCTA), 2018, pp. 1526–1531, https://doi.org/10.1109/CCTA.2018.8511529.
[34] W. Waag, S. Käbitz, D.U. Sauer, Application-specific parameterization of reduced order equivalent circuit battery models for improved accuracy at dynamic load, Measurement 46 (2013) 4085–4093, https://doi.org/10.1016/j.measurement.2013.07.025.
[35] Y. Hu, S. Yurkovich, Y. Guezennec, B.J. Yurkovich, A technique for dynamic battery model identification in automotive applications using linear parameter varying structures, Control. Eng. Pract. 17 (10) (2009) 1190–1201.
[36] Y. Hu, S. Yurkovich, Y. Guezennec, B.J. Yurkovich, Electro-thermal battery model identification for automotive applications, J. Power Sources 196 (1) (2011) 449–457, https://doi.org/10.1016/j.jpowsour.2010.06.037.
[37] X. Hua, C. Zhang, G. Offer, Finding a better fit for lithium ion batteries: a simple, novel, load dependent, modified equivalent circuit model and parameterization method, J. Power Sources 484 (2021), 229117, https://doi.org/10.1016/j.jpowsour.2020.229117.
[38] W. Allafi, K. Uddin, C. Zhang, R.M.R.A. Sha, J. Marco, On-line scheme for parameter estimation of nonlinear lithium ion battery equivalent circuit models using the simplified refined instrumental variable method for a modified wiener continuous-time model, Appl. Energy 204 (2017) 497–508.
[39] A. Barai, W.D. Widanage, J. Marco, A. McGordon, P. Jennings, A study of the open circuit voltage characterization technique and hysteresis assessment of lithium-ion cells, J. Power Sources 295 (2015) 99–107.
[40] M. Ouyang, G. Liu, L. Lu, J. Li, X. Han, Enhancing the estimation accuracy in low state-of-charge area: a novel onboard battery model through surface state of charge determination, J. Power Sources 270 (2014) 221–237.
[41] A. Malik, Z. Zhang, R.K. Agarwal, Extraction of battery parameters using a multi-objective genetic algorithm with a non-linear circuit model, J. Power Sources 259 (2014) 76–86, https://doi.org/10.1016/j.jpowsour.2014.02.062.
[42] A. Klintberg, T. Wik, B. Fridholm, Theoretical bounds on the accuracy of state and parameter estimation for batteries, in: 2017 American Control Conference (ACC), 2017, pp. 4035–4041.